2011 50th IEEE Conference on Decision and Control and
European Control Conference (CDC-ECC)
Orlando, FL, USA, December 12-15, 2011

Real-Time Sliding Mode Control for a Doubly Fed Induction Generator

R. Ruiz, E. N. Sanchez and A. G. Loukianov

Abstract— **This paper proposes a control scheme based on the block control technique using sliding modes, for a doubly fed induction generator (DFIG) prototype connected to an infinity bus. The DFIG is widely used as a wind generator; it allows the rotor speed to vary while synchronizing the stator directly to a fixed frequency power system. The generation scheme for the DFIG has one back-to-back PWM voltage-source converter connected between the rotor and the electrical grid. The rotor side converter (RSC) is connected via a dc link to the grid side converter (GSC), which is in turn connected to the stator terminals directly or through a step-up transformer. A block control scheme for the RSC is proposed to control the electric torque and the reactive power independently. The variables to be controlled by the GSC are the dc voltage in the dc link and the reactive power in the step-up terminals. The performance of the control scheme proposed is illustrated via real-time implementation in a 1/4HP DFIG prototype.**

I. Introduction

Wind energy, compared with fossil fuels, is plentiful, renewable, widely distributed, clean, and produces no greenhouse gas emissions. Wind power is the conversion of wind energy into a useful form of energy, such as using wind turbines to produce electricity. Within the range of generators used in the wind energy, the Doubly Fed Induction Generator is widely used as a wind generator; it allows the rotor speed to vary while synchronizing the stator directly to a fixed frequency power system. This is achieved by controlling the rotor magnetic field by means of rotor currents supplied from a rotor side converter as illustrated in Fig. 1. The RSC is connected via a dc link to a grid side converter, which is in turn connected to the stator terminals directly or through a step-up transformer. Both RSC and GSC are four-quadrant converters which allow bi-directional flow of power; different techniques have been proposed for this configuration control. In [1], using Integral Sliding Modes, a tracking control is proposed for electric torque and reactive power in order to maintain a constant stator power factor. In [2], using a non-coupled vector control technique, a PI stator current controller is designed for active and reactive power control. In [3], an exact feedback linearization technique is applied to design a non-linear controller, considering a utility bus voltage change as a disturbance. In [4], a block control scheme with sliding modes is used to design a control for rotor speed tracking and to keep the stator power factor constant by means of the stator reactive power output; however, that publication presents the RSC controller only, and the simulations results neglect the IGBT's dynamics.

R. Ruiz, E. N. Sanchez and A. G. Loukianov are with CINVESTAV-IPN, Campus Guadalajara, Av. del Bosque 1145, Col. El Bajío, Zapopan, C.P. 45019, Jalisco, México. Phone: +52-33-3777-3600 Fax: +52-33-3777-3609 Email: [rruiz][sanchez][louk]@gdl.cinvestav.mx

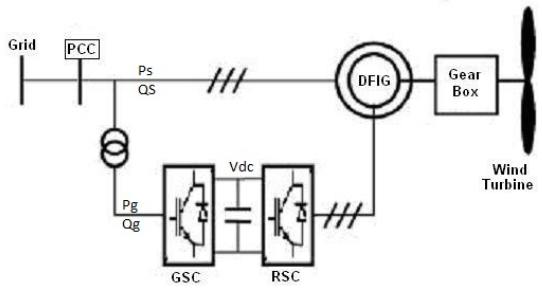

Fig. 1. Variable speed DFIG with IGBT converter

In [5], optimal PI controllers were designed using particle swarm optimization. In the present paper, the authors propose a block control scheme using sliding modes, for the RSC and the GSC of a doubly fed induction generator connected to an infinity bus. The variables to be controlled by the RSC are the electric torque (T_e) and the stator reactive power (Q_s), and the ones for the GSC are the dc voltage (V_{dc}) in the dc link and the reactive power in the step-up terminals (Q_g).

II. Discrete-Time Mathematical Model

A. Double Fed Induction Generator

The DFIG rotor and stator three phase windings are assumed to be symmetrical and balanced, and the rotor speed can be below or above the synchronous speed of the stator flux [6]. The discrete-time equations for the DFIG are developed in per unit as[4]:

$$\omega_r(k+1) = \omega_r(k) + \tau\frac{1}{2H}(T_m(k) - T_e(k)), \qquad (1)$$

$$\begin{aligned} i_s(k+1) = & i_s(k) + \tau(A_{11}(k)i_s(k) + A_{12}(k)i_r(k)) \\ & + \tau(D_1 v_s(k) + B_2 u(k)), \end{aligned} \qquad (2)$$

$$\begin{aligned} i_r(k+1) = & i_r(k) + \tau(A_{21}(k)i_s(k) + A_{22}(k)i_r(k)) \\ & + \tau(D_2 v_s(k) + B_2 u(k)), \end{aligned} \qquad (3)$$

$$T_e(k) = i_r(k)^T M_{T_e} i_s(k), \qquad (4)$$

where

$$i_s(k) = \begin{bmatrix} i_{ds}(k) \\ i_{qs}(k) \end{bmatrix}, i_r(k) = \begin{bmatrix} i_{dr}(k) \\ i_{qr}(k) \end{bmatrix},$$

$$v_s(k) = \begin{bmatrix} v_{ds}(k) \\ v_{qs}(k) \end{bmatrix}, u(k) = \begin{bmatrix} v_{dr}(k) \\ v_{qr}(k) \end{bmatrix},$$

978-1-61284-799-3/11/$26.00 ©2011 IEEE

$$A_{11}(k)=\begin{bmatrix} -\frac{\omega_b R_s}{X_s\sigma} & \omega_b\left(1-\frac{\sigma-1}{\sigma}\omega_r(k)\right) \\ -\omega_b\left(1-\frac{\sigma-1}{\sigma}\omega_r(k)\right) & -\frac{\omega_b R_s}{X_s\sigma}\end{bmatrix},$$

$$A_{12}(k)=\begin{bmatrix} -\frac{\omega_b X_m R_r}{X_s X_r\sigma} & -\frac{\omega_b X_m}{X_s\sigma}\omega_r(k) \\ \frac{\omega_b X_m}{X_s\sigma}\omega_r(k) & -\frac{\omega_b X_m R_r}{X_s X_r\sigma}\end{bmatrix},$$

$$B_1=\begin{bmatrix} \frac{\omega_b X_m}{X_s X_r\sigma} & 0 \\ 0 & \frac{\omega_b X_m}{X_s X_r\sigma}\end{bmatrix}, D_1=\begin{bmatrix} -\frac{\omega_b}{X_s\sigma} & 0 \\ 0 & -\frac{\omega_b}{X_s\sigma}\end{bmatrix},$$

$$A_{21}(k)=\begin{bmatrix} -\frac{\omega_b X_m R_s}{X_s X_r\sigma} & \frac{\omega_b X_m}{X_r\sigma}\omega_r(k) \\ -\frac{\omega_b X_m}{X_r\sigma}\omega_r(k) & -\frac{\omega_b X_m R_s}{X_s X_r\sigma}\end{bmatrix},$$

$$A_{22}(k)=\begin{bmatrix} -\frac{\omega_b R_r}{X_r\sigma} & \omega_b(1-\frac{1}{\sigma}\omega_r(k)) \\ -\omega_b(1-\frac{1}{\sigma}\omega_r(k)) & -\frac{\omega_b R_r}{X_r\sigma}\end{bmatrix},$$

$$D_2=\begin{bmatrix} -\frac{\omega_b X_m}{X_s X_r\sigma} & 0 \\ 0 & -\frac{\omega_b X_m}{X_s X_r\sigma}\end{bmatrix}, B_2=\begin{bmatrix} \frac{\omega_b}{X_r\sigma} & 0 \\ 0 & \frac{\omega_b}{X_r\sigma}\end{bmatrix},$$

$$\sigma=1-\frac{X_m^2}{X_s X_r},\ M_{T_e}=X_m\begin{bmatrix} 0 & 1 \\ -1 & 0\end{bmatrix},$$

and ω_b is the base angular speed, ω_r is the rotor speed (pu),i_{ds} ,i_{qs}, i_{dr}, i_{qr} are the stator and rotor currents in the d and q axes respectively (pu), v_{ds} ,v_{qs}, v_{dr}, v_{qr} are the stator and rotor voltages in the d and q axes respectively (pu), T_e is the electromagnetic torque (pu), T_m is the mechanical torque (pu), X_s is the stator self-reactance per phase (pu), X_r is the rotor self-reactance per phase (pu), X_m is the magnetization reactance (pu), R_s is the stator resistance per phase (pu), R_r is the rotor resistance per phase (pu), H is the moment of inertia (sec) and τ is the sampling time.

B. DC Link

The GSC is connected to the grid source through a step-up transformer. The GSC works like a rectifier to keep the dc voltage constant in the dc link and to allow bi-directional power flow. The discrete-time equations in per unit for the DC link are defined as:

$$V_{dc}(k+1)=V_{dc}(k)+\tau\left(\frac{1}{CV_{dc}(k)}v_{gs}^T(k)M_P i_g(k)\right), \quad (5)$$

$$i_g(k+1)=i_g(k)+\tau(A_g i_g(k)+B_g v_{gs}(k)-B_g u_g(k)), \quad (6)$$

with $V_{dc}(0)\neq 0$, where

$$A_g=\begin{bmatrix} -\frac{\omega_b R_g}{X_l} & \omega_s \\ -\omega_s & -\frac{\omega_b R_g}{X_l}\end{bmatrix}, B_g=\begin{bmatrix} \frac{\omega_b}{X_l} & 0 \\ 0 & \frac{\omega_b}{X_l}\end{bmatrix},$$

$$M_P=\begin{bmatrix} 1 & 0 \\ 0 & 1\end{bmatrix},$$

$$i_g=\begin{bmatrix} i_{dg} \\ i_{qg}\end{bmatrix}, v_{gs}=\begin{bmatrix} v_{dgs} \\ v_{qgs}\end{bmatrix}, u_g=\begin{bmatrix} v_{dg} \\ v_{qg}\end{bmatrix},$$

and, ω_s is the synchrony frequency (rad/sec), i_{dg}, i_{qg} are the currents in the d and q axes respectively (pu), v_{dgs}, v_{qgs}, v_{dg}, v_{qg} are the step-up transformer and GSC voltages in the d and q axes respectively (pu), R_g is the resistance of the three phase lines a, b, c (pu), X_l is the reactance of three phase lines a, b, c (pu), C is the capacitance of the dc link (pu) and τ is the sampling time.

III. RSC Controller Design

The variables to be controlled are the DFIG electric torque $T_e(k)$ and the stator reactive power $Q_s(k)$. The control objectives are: a) to track a time-varying electric torque trajectory $T_e^{ref}(k)$, and b) to keep constant the electric power factor $f_{ps1}(k)$ at the stator terminals by means of the stator reactive power $Q_s(k)$ control. The electric torque $T_e(k)$ and stator reactive power $Q_s(k)$ are defined respectively as (4), and

$$Q_s(k)=v_s(k)^T M_Q i_s(k), \quad (7)$$

where $M_Q=\begin{bmatrix} 0 & -1 \\ 1 & 0\end{bmatrix}$.

The reference for reactive power is defined as a function of electric power factor f_{ps1} [7]:

$$Q_s^{ref}(k)=\frac{P_s(k)}{f_{ps1}}\sqrt{1-f_{ps1}^2}, \quad (8)$$

where $P_s(k)\approx\omega_{sync}T_e(k)$.

Analyzing the steady state of the system (2) and (3), the following equations are obtained:

$$i_r(k)=G_1 i_s(k)+H_1 v_s(k), \quad (9)$$

$$i_s(k)=G_2 i_r(k)+H_2 v_s(k), \quad (10)$$

where

$$G_1=\begin{bmatrix} \frac{X_s}{X_m} & \frac{R_s}{X_m} \\ -\frac{R_s}{X_m} & \frac{X_s}{X_m}\end{bmatrix}, H_1=\begin{bmatrix} 0 & \frac{1}{X_m} \\ -\frac{1}{X_m} & 0\end{bmatrix},$$

$$G_2=\begin{bmatrix} \frac{X_m X_s}{R_s^2+X_s^2} & -\frac{X_m R_s}{R_s^2+X_s^2} \\ \frac{X_m R_s}{R_s^2+X_s^2} & \frac{X_m X_s}{R_s^2+X_s^2}\end{bmatrix},$$

$$H_2=\begin{bmatrix} -\frac{R_s}{R_s^2+X_s^2} & -\frac{X_s}{R_s^2+X_s^2} \\ \frac{X_s}{R_s^2+X_s^2} & -\frac{R_s}{R_s^2+X_s^2}\end{bmatrix}.$$

In order to simplify the controller synthesis, we assume that (9) and (10) are approximately valid during transient; thus (2) and (3) can be rewritten using (9) and (10), as:

$$i_s(k+1)=f_{i_s}(k)+\tau B_1 u(k), \quad (11)$$

$$i_r(k+1)=f_{i_r}(k)+\tau B_2 u(k), \quad (12)$$

where

$$f_{i_s}(k)=i_s(k)+\tau\left(A_{11}(k)+A_{12}(k)G_1\right)i_s(k)+\tau\left(A_{12}(k)H_1+D_1\right)v_s(k),$$

$$f_{i_r}(k)=i_r(k)+\tau\left(A_{21}(k)G_2+A_{22}(k)\right)i_r(k)+\tau\left(A_{21}(k)H_2+D_2\right)v_s(k).$$

Evaluating (4) at $(k+1)$ and using (11) and (12), $T_e(k+1)$ is defined as

$$T_e(k+1)=f_{T_e}(k)+B_{T_e}(k)u(k), \quad (13)$$

where

$$f_{T_e}(k)=f_{i_r}(k)^T M_{T_e} f_{i_s}(k),$$

$$B_{T_e}(k) = \tau(f_{i_s}(k)^T M_{T_e}^T B_2 + f_{i_r}(k)^T M_{T_e} B_1).$$

Evaluating (7) at $(k+1)$ and using (11), then

$$Q_s(k+1) = f_{Q_s}(k) + B_{Q_s}(k)\, u(k), \tag{14}$$

where

$$f_{Q_s}(k) = v_s(k)^T M_Q f_{i_s}(k),$$

$$B_{Q_s}(k) = \tau v_s(k)^T M_Q B_1.$$

From (13) and (14), the following system is formulated

$$x_1(k+1) = f_{x_1}(k) + B_{x_1}(k)u(k), y(k) = x_1(k), \tag{15}$$

where

$$x_1(k) = \begin{bmatrix} T_e(k) \\ Q_s(k) \end{bmatrix},\ f_{x_1}(k) = \begin{bmatrix} f_{T_e}(k) \\ f_{Q_s}(k) \end{bmatrix},$$

$$B_{x_1}(k) = \begin{bmatrix} B_{T_e}(k) \\ B_{Q_s}(k) \end{bmatrix}.$$

The sliding manifold is defined as:

$$s(k) = x_1(k) - x_1^{ref}(k), \tag{16}$$

where $x_1^{ref}(k) = \begin{bmatrix} T_e^{ref}(k) \\ Q_s^{ref}(k) \end{bmatrix}$.
Evaluating (16) at $(k+1)$, the equivalent control $u^{equ}(k)$ is calculated as [8]:

$$u^{equ}(k) = -\frac{1}{\tau} B_{x_1}(k)^{-1} (f_{x_1}(k) - x_1^{ref}(k+1)). \tag{17}$$

Applying $u(k) = u^{equ}(k)$ to (15), the state of the closed-loop system reaches the sliding manifold $s(k) = 0$ in one sampling period. However, it is appropriate to add to the control signal a stabilizing term $u^{din}(k)$, defined as:

$$u^{din}(k) = \frac{1}{\tau} B_{x_1}(k)^{-1} (Ks(k) + K_0 s_0(k)), \tag{18}$$

where $Ks(k)$ is included in order to reach the sliding surface asymptotically and to avoid high gain control, $K_0 s_0(k)$ is an integral term to reject the unmodeled dynamics and to reduce the steady state error; additionally K_s, K_0 should be selected such that $\begin{bmatrix} I & \tau I \\ K_0 & K \end{bmatrix}$ is a Schur matrix [9]. The integral term $s_0(k)$ is defined as:

$$s_0(k+1) = s_0(k) + \tau s_1(k). \tag{19}$$

Hence, the complete control $u^c(k)$ is proposed as

$$u^c(k) = u^{equ}(k) + u^{din}(k). \tag{20}$$

To take into account the boundedness of the control signal $\|u(k)\| < u_{\max}$, $u_{\max} > 0$, the following control law is selected [8]:

$$u(k) = \begin{cases} u_{\max} \frac{u^c(k)}{\|u^c(k)\|} & if\ \|u^c(k)\| > u_{\max} \\ u^c(k) & if\ \|u^c(k)\| \le u_{\max} \end{cases} \tag{21}$$

IV. GSC Controller Design

The variables to be controlled are the capacitor voltage $V_{dc}(k)$ and the reactive power $Q_g(k)$. The control objectives are: a) to track a dc voltage reference $V_{dc}^{ref}(k)$ in the dc link, and b) to keep constant the electric power factor $f_{ps2}(k)$ at the step-up transformer terminals by means of the reactive power $Q_g(k)$ control.
The step-up transformer reactive power $Q_g(k)$ is defined as:

$$Q_g(k) = v_{sg}(k)^T M_Q i_g(k). \tag{22}$$

The reference for the reactive power is defined as a function of electric power factor f_{ps2} [7]:

$$Q_g^{ref}(k) = \frac{P_g(k)}{f_{ps2}} \sqrt{1 - f_{ps2}^2}. \tag{23}$$

Let define the tracking error for the dc voltage as

$$\varepsilon_1^g(k) = V_{dc}(k) - V_{dc}^{ref}(k). \tag{24}$$

From (24), using (5), then $\varepsilon_1^g(k+1)$ is equal to

$$\begin{aligned} \varepsilon_1^g(k+1) = V_{dc}(k) + \tau \left(\tfrac{1}{CV_{dc}(k)} v_{gs}^T(k) M_P i_g(k) \right) \\ -V_{dc}^{ref}(k+1), \end{aligned} \tag{25}$$

and considering that in the dq axes $v_{qg}(k) = 0$, the dc voltage is controlled directly by $i_{dg}(k)$

$$\begin{aligned} \varepsilon_1^g(k+1) = V_{dc}(k) + \tfrac{\tau}{CV_{dc}(k)} v_{dgs}(k) i_{dg}(k) \\ -V_{dc}^{ref}(k+1). \end{aligned} \tag{26}$$

Then, the i_{dg} reference is defined as

$$\begin{aligned} i_{dg}^{ref}(k) = \frac{2CV_{dc}(k)}{3\tau V_{ds}(k)} (V_{dc}^{ref}(k+1) - V_{dc}(k) \\ +k_1 \varepsilon_1^g(k) + k_0 \varepsilon_0^g(k)), \end{aligned} \tag{27}$$

where $\begin{bmatrix} 1 & \tau \\ k_0 & k_1 \end{bmatrix}$ is a Schur matrix [9], $k_1 \varepsilon_1^g(k)$ is introduced to reach the reference asymptotically; in order to reject the unmodeled dynamics and reduce the steady state error a integral term $k_0 \varepsilon_0^g(k)$ is inserted:

$$\varepsilon_0^g(k+1) = \varepsilon_0^g(k) + \tau \varepsilon_1^g(k). \tag{28}$$

On the other hand, the tracking error for the reactive power is

$$\varepsilon_2^g(k) = Q_g(k) - Q_g^{ref}(k). \tag{29}$$

From (22), and considering that $v_{qgs}(k) = 0$, it could be established

$$Q_g(k) = -v_{dgs}(k) i_{qg}(k). \tag{30}$$

Assuming $\varepsilon_2^g(k) = 0$, then $Q_g(k) = Q_g^{ref}(k)$; therefore, it is easy to see that i_{qg}^{ref} is given by:

$$i_{qg}^{ref}(k) = -i_{dg}(k) \frac{\sqrt{1 - f_{ps2}^2}}{f_{ps2}}. \tag{31}$$

Then the sliding manifold is formulated as:

$$s_g(k) = i_g(k) - i_g^{ref}(k), \tag{32}$$

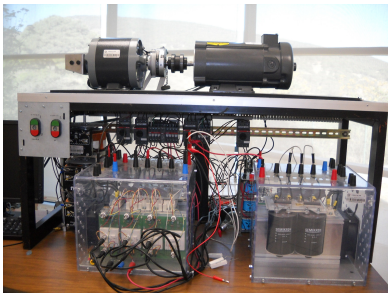

Fig. 2. DFIG Prototype

where $i_g^{ref}(k) = \begin{bmatrix} i_{dg}^{ref}(k) \\ i_{qg}^{ref}(k) \end{bmatrix}$.

Evaluating (32) at $(k+1)$, the equivalent control $u_g^{equ}(k)$ is calculated as [8]:

$$u_g^{equ}(k) = -\frac{1}{\tau} B_g^{-1}(i_g(k) + \tau(A_g i_g(k) + B_g v_{gs}(k)) - i_g^{ref}(k+1)). \quad (33)$$

Applying $u(k) = u_g^{equ}(k)$ to (6), the state of the closed-loop system reaches the sliding manifold $s_g(k) = 0$ in one sampling period. However, it is appropriate to add to the control signal a stabilizing term $u_g^{din}(k)$ in order to reach the sliding surface asymptotically and to avoid high gain control; hence, the complete control $u_g^c(k)$ is proposed as:

$$u_g^c(k) = u_g^{equ}(k) + u_g^{din}(k), \quad (34)$$

where

$$u_g^{din}(k) = \frac{1}{\tau} B_g(k)^{-1} (K_g s_g(k) + K_{0g} s_{0g}(k)), \quad (35)$$

$K_g = \begin{bmatrix} k_1^g & 0 \\ 0 & k_2^g \end{bmatrix}$, $K_{0g} = \begin{bmatrix} 0 \\ k_0^g \end{bmatrix}$; in order to reject the unmodeled dynamics and reduce the steady state error, the integral term $s_{0g}(k)$ is inserted, defined as

$$s_{0g}(k+1) = s_{0g}(k) + \tau \left(i_{qg}(k) - i_{qg}^{ref}(k) \right), \quad (36)$$

and $\begin{bmatrix} k_1^g & 0 & 0 \\ 0 & 1 & \tau \\ 0 & k_0^g & k_2^g \end{bmatrix}$ is a Schur matrix [9]. To take into account the boundedness of the control signal $\|u_g(k)\| < u_{g\max}$, $u_{g\max} > 0$, the following control law is selected [8]:

$$u_g(k) = \begin{cases} u_{g\max} \frac{u_g^c(k)}{\|u_g^c(k)\|} & if \ \|u_g^c(k)\| > u_{g\max} \\ u_g^c(k) & if \ \|u_g^c(k)\| \le u_{g\max} \end{cases} \quad (37)$$

V. Real-Time Results

To evaluate the performance of the proposed RSC and GSC controllers a real-time implementation in a 1/4HP three-phase generator prototype is developed; it is shown in Fig.2. The DFIG prototype parameters appear in Table I. The implementation is performed using Simulink/MATLAB[1] with a data adquisition board DS1104[2]. The Wind Turbine is emulated by a 3/4HP DC motor. In this paper two case studies are presented: a) constant wind turbine speed with a time-varying electric torque reference, and b) constant electric torque reference with a time-varying wind turbine speed.

[1]Simulink/MATLAB is a trademark of MathWorks.
[2]DS1104 R&D Controller Board of dSPACE GmbH

Symbol	Parameter	Value
X_m	Magnetizing Reactance	$2.3175pu$
X_s	Stator Reactance	$2.4308pu$
X_r	Rotor Reactance	$2.4308pu$
R_s	Stator Windings Resistance	$0.1609pu$
R_r	Rotor Windings Resistance	$0.0502pu$
H	Angular Moment of Inertia	$0.23sec$
ω_b	Base Angular Frequency	$376.99112rad/sec$
P_b	Base Power	$185.4VA$
V_b	Base Voltage	$179.63V$
X_l	Three Phase Lines Reactance	$0.0045pu$
R_g	Three Phase Lines Resistance	$0.0014pu$
C	DC Link Capacitance	$0.1854pu$

TABLE I
Parameters of Double Fed Induction Generator Prototype

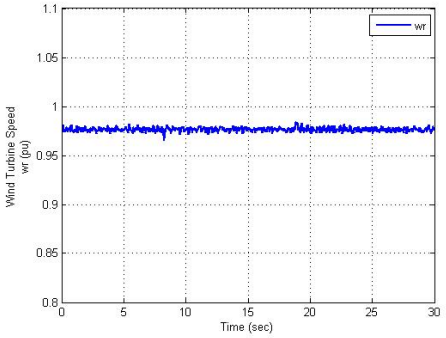

Fig. 3. Case a, wind turbine speed

A. Constant Wind Turbine Speed

The real-time implementation conditions for the first case are:

- Time lapse: 30 seconds.
- Sampling time step: $500\mu s$.
- Constant Wind Turbine speed: $0.97pu$.
- Initial RSC Controller references: $T_e^{ref} = 0.5pu$, $f_{ps} = 1$ ($Q_s^{ref} = 0pu$).
- At 8.15 seconds, a change to $T_e^{ref} = 0.9pu$ is incepted.
- At 18.83 seconds, $T_e^{ref} = 0.5pu$ is incepted again.
- GSC controller references: $V_{dc}^{ref} = 0.55pu$, $f_{ps} = 1$ ($Q_g^{ref} = 0pu$).

The wind turbine speed emulated by the DC motor is shown in Fig. 3. As a first step the wind turbine speed is assumed constant to focus on the electric torque tracking. The performance of the RSC controller is presented in Fig. 4 and Fig. 5. Fig 4 displays the output variables T_e and Q_s for the RSC; it can seen that the electric torque and the reactive power tracking is achieved. The power factor and the RSC control signals v_{dr}, v_{qr} are presented in Fig. 5; it is possible to see that the control signals are bounded. The controlled output variables V_{dc}, Q_g for the GSC are displayed in Fig.

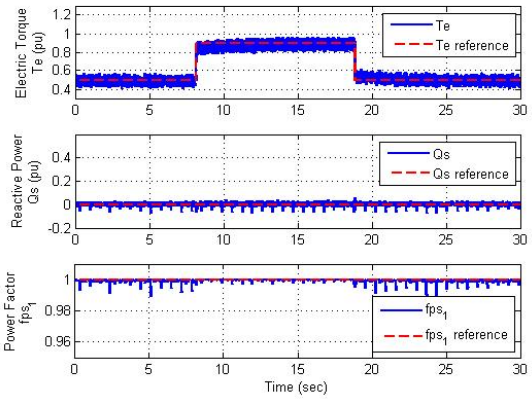

Fig. 4. Case a, T_e, Q_s and f_{ps1} as controlled by the RSC

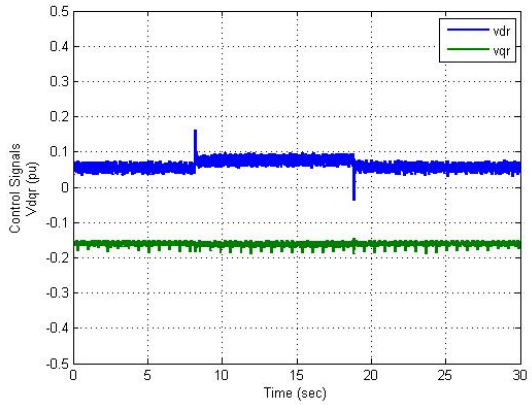

Fig. 5. Case a, RSC control signals v_{dr}, v_{qr}

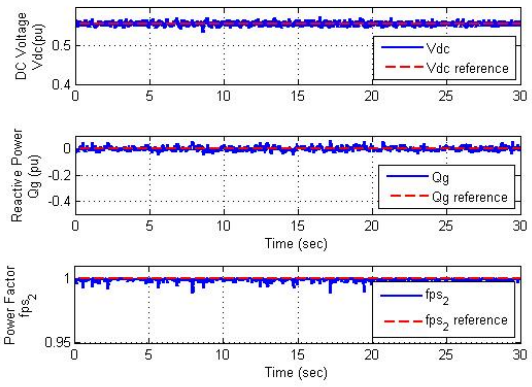

Fig. 6. Case a, V_{dc}, Q_g and f_{ps2} controlled by the GSC

6; the GSC control signals v_{dg}, v_{qg} are shown in Fig. 7. It is ease to see, that both RSC and GSC block controllers reach the control objective with a small tracking error. The generator output voltage spectrum is shown in Fig. 8, where it can be seen that it does not have harmonic frequencies.

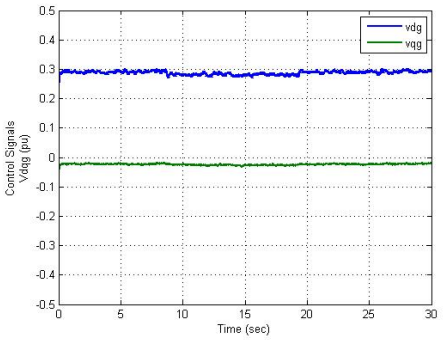

Fig. 7. Case a, GSC control signals v_{dg}, v_{qg}

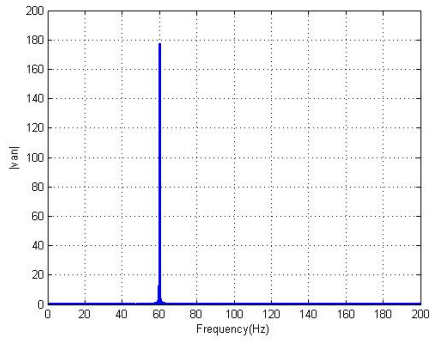

Fig. 8. Case a, grid voltage spectrum

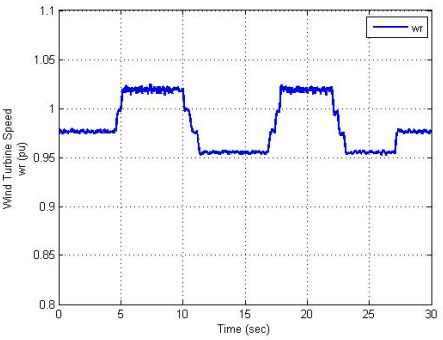

Fig. 9. Case b, wind turbine speed

B. Constant Electric Torque

The real-time implementation conditions for the second case are:

- Time lapse: 30 seconds.
- Sampling time step: $500\mu s$.
- RSC controller references: $T_e^{ref} = 0.5pu$, $f_{ps} = 1$ ($Q_s^{ref} = 0pu$).
- GSC controller references: $V_{dc}^{ref} = 0.55pu$, $f_{ps} = 1$ ($Q_g^{ref} = 0pu$).
- Wind Turbine speed changes between $0.95pu$ to $1.02pu$.

The wind turbine speed changes is shown in Fig. 9. Fig. 10 presents the output variables T_e and Q_s controlled for the RSC, and it can see that the effect of speed changes in the electric torque and reactive power tracking are small. The

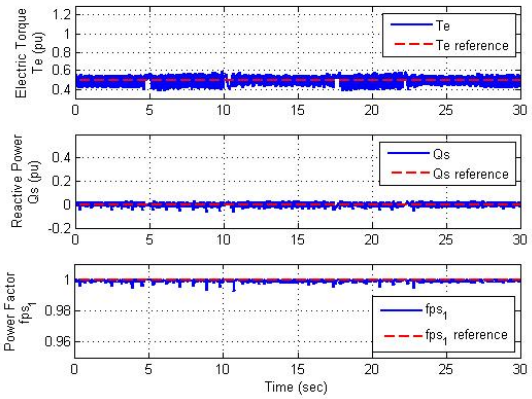

Fig. 10. Case b, T_e, Q_s and f_{ps1} controlled by the RSC

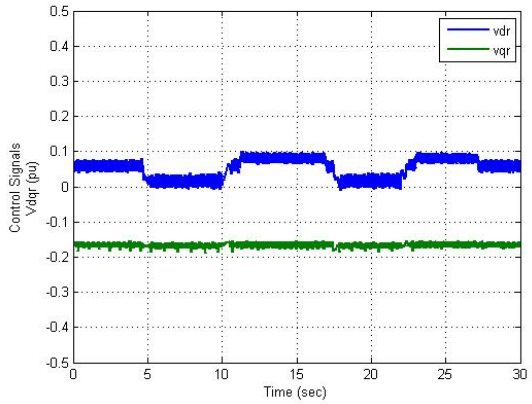

Fig. 11. Case b, RSC control signals v_{dr}, v_{qr}

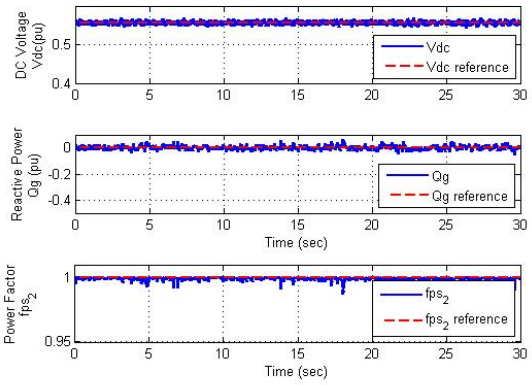

Fig. 12. Case b, V_{dc}, Q_g and f_{ps2} controlled by the GSC

speed changes has not a significant effect to power factor, as can be seen in Fig. 10. The speed changes are compensated for the control signals, Fig. 11. The performance of the GSC controller is present in Fig. 12 and Fig. 13. The effect of the speed change is not presented in the output variables V_{dc} and Q_g of the GSC controller. The RSC and GSC block controllers reaches the objective in this case too.

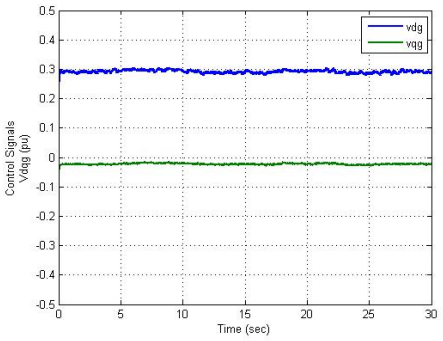

Fig. 13. Case b, GSC control signals v_{dg}, v_{qg}

VI. Conclusions

This paper has developed a block control scheme, using sliding modes, for a doubly fed induction generator, which is implemented in a real-time. Discrete-time sliding modes for RSC are used to track a reference trajectory for the electric torque T_e and to keep constant the electric power factor f_{ps1}; for the GSC, discrete-time sliding modes are used to keep the dc voltage V_{dc} constant and to keep constant the electric power factor f_{ps2} in the step-up transformer. The generator rotor speed ω_r is controlled by a DC motor which is not described in this paper. For case a; the electric torque and the reactive power tracking is succesfull for a time-varying electric torque reference; for case b; it can be seen that the proposed control scheme reaches the objective even in presence of speed changes in the wind turbine speed and unmodeled dynamics.

References

[1] O. A. Morfin, A. G. Loukianov, and J. M. Cañedo, "Robust non-linear control of a wound rotor induction generator: integral sliding modes," *North American Power Symposium (NAPS)*, September 2008.

[2] R. Peña, J. C. Clare, and G. M. Asher, "Doubly fed induction generator using back to back pwm converters and its application to variable speed wind energy generation," *IEEE Proceedings Electric Power Applications*, vol. 143, no. 3, pp. 231–241, May 1996.

[3] P. N. Lan, N. P. Quang, and P. Buechner, "A non-linear control algorithm for improving performance of wind generator using doubly-fed induction generator," *European Wind Energy Conference and Exhibition*, May 2006.

[4] R. Ruiz, E. N. Sánchez, and A. G. Loukianov, "Discrete time block control of a double fed induction generator using sliding modes," *IEEE Multi-conference on Systems and Control (MSC)*, July 2009.

[5] W. Qiao, G. K. Venayagamoorthy, and R. G. Harley, "Design of optimal pi controllers for doubly fed induction generators driven by wind turbines using particle swarm optimization," *International Joint Conference on Neural Networks*, pp. 1982–1987, July 2006.

[6] T. Burton, D. Sharpe, N. Jenkis, and E. Bossanyi, *Wind Energy Handbook*. New York, USA: John Wiley and Sons, 2001.

[7] A. Tapia, G. Tapia, J. X. Estolaza, and J. R. Saenz, "Modeling and control of a wind turbine driven doubly fed induction generator," *IEEE Transactions on Energy Conversion*, vol. 26, no. 2, pp. 194–204, June 2003.

[8] V. Utkin, J. Guldner, and J. Shi, *Sliding Mode Control in Electromechanical Systems*. Taylor and Francis, 1999.

[9] A. Varga, "A schur method for pole assigment," *IEEE Transactions on Automatic Control*, vol. 26, no. 2, pp. 517–519, 1981.